J. Condensed Matter Nucl. Sci. 15 (2015) 231–239

Research Article

A Mass-Flow-Calorimetry System for Scaled-up Experiments on Anomalous Heat Evolution at Elevated Temperatures

A. Kitamura*,†, A. Takahashi‡, R. Seto and Y. Fujita
Technova Inc., Japan

A. Taniike and Y. Furuyama
Kobe University, Japan

Abstract

A new mass-flow calorimetry system has been installed to investigate the excess-power phenomena at elevated temperatures with an increased amount of the sample. Calibration runs using alumina powder has revealed very good stability with very high heat recovery rate. The first trial runs with a silica-included Cu·Ni nano-composite sample containing 4 g of Ni mixed with 200 g of Al_2O_3 showed an anomalous increase in temperature of the sample, which could imply a long-lasting excess power of 5 W/g-Ni.
 ISSN 2227-3123

Keywords: Hydrogen gas absorption, Oil-cooling mass-flow calorimetry, Silica-included Cu·Ni nano-composite, 5 W/g-Ni

1. Introduction

We have been studying phenomena of anomalous heat evolution from hydrogen-isotope-loaded nano-composite samples at elevated temperatures as well as at room temperature using a $A_1 \cdot A_2$ twin absorption system [1,2]. Recent experiments have used Ni-based nano-composite samples; Pd_1Ni_7/ZrO_2 ("PNZ"), Ni/ZrO_2 ("NZ"), $Cu_{0.081}Ni_{0.36}/ZrO_2$ ("CNZ") and $Cu_{0.21}Ni_{0.21}/ZrO_2$ ("CNZII"). The results of measurements have been presented in the 12th Annual Meeting of the Japan CF-Research Society (JCF12), the 17th International Conference on Condensed Matter Nuclear Science (ICCF17) and the 13th Annual Meeting of the Japan CF-Research Society (JCF13), and have been/will be published in [3–5], respectively.

These are summarized, and the time-dependent data are re-analysed in another paper by A. Takahashi in this Conference [6] in a paper speculating about heat releasing mechanisms during the several-weeks-long phase of D(H)-loading into the nano-composite samples. As shown there, many interesting, even astonishing, features are involved:

*E-mail: kitamuraakira3@gmail.com
†Also at: Kobe University, Japan.
‡Also at: Osaka University, Japan.

 ISSN 2227-3123

burst-like heat release with anomalously high values of differential heat of sorption (η) reaching about 600 eV/atom-H; large values of integrated heat reaching about 800 eV/atom-Ni from the CNZ sample absorbing H; and abrupt desorption with absorbed energy of 50–80 eV/atom-Ni observed almost exclusively in the first 573-K run for each sample.

To confirm these interesting phenomena, repeated measurements with improved signal-to-noise ratio are required. Since the easiest way to accomplish this is to increase the amount of sample material being tested, we have fabricated a reaction chamber with ten-times-larger volume than the present one. Another important improvement is mass flow calorimetry applied to the system using an oil coolant with a boiling point of 390°C.

In the present paper we show the characteristics of this new oil-cooling mass-flow calorimetry system for observing anomalous heat evolution in H-gas charging to Ni-based nano-composite samples and for calibration runs using blank alumina sample.

2. Description of the System

The improvement has been done on the A_2 part of the $A_1 \cdot A_2$ twin system. The reaction chamber (RC) with a capacity of 50 cm^3 has been replaced with one with a capacity of 500 cm^3. A schematic of this new system, called the "C_1 system", is shown in Fig. 1.

On the outer surface of the RC, a coolant pipe and a 1-kW sheath heater are wound alternately for heat removal

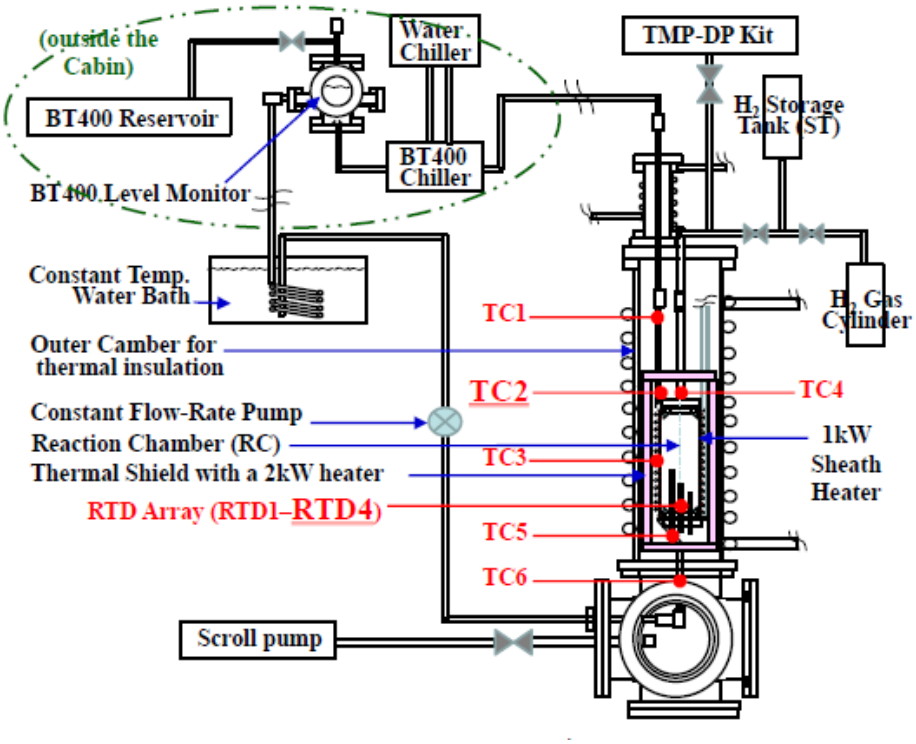

Figure 1. Schematic of the C_1 absorption system.

and sample heating, respectively. These are enclosed by a thin sheet of stainless steel for the purpose of thermal shield and close contact of the sheath heater to the side surface of the RC. All of these are supported by a stainless-steel pipe feeding H_2 gas to the sample in the RC, and surrounded again by a thermal shield made of ceramic fiber (Isowool 14C; Isolite Insulating Products Co. Ltd.) not only on the side but also on the top and the bottom. The power to the heater is fed from a DC power supply in a constant-current mode.

The coolant oil is an aromatic hydrocarbon (Barreltherm-400; Matsumura oil Co. Ltd.), which has a boiling point of 390°C and a practical maximum temperature of 330°C. The coolant is driven by a digital liquid tubing pump (Masterflex peristaltic pump) with a constant flow rate of 20 cm^3/min or 40 cm^3/min in the present work. The plastic peristaltic tube (the section that is squeezed by the rotor) is either Viton or Tygon. The coolant is fed to the RC from the bottom, and heated by the heater and the H-absorbing sample. After emerging from the top flange, the oil is cooled down to the ambient temperature, and fed back to the tubing pump through a water bath kept at a temperature of 24.0±0.1°C.

Seven thermocouples (TC) are deployed; 5 points on the surface of the coolant pipe; TC1, TC2, TC3, TC5 and TC6, on the gas feed pipe TC4, and TC0 for monitoring the ambient temperature. For flow calorimetry TC2 just behind the outlet from the RC is used. In addition to the TC's, four resistance temperature detectors (RTD; 3-terminal type) are deployed inside the RC to directly measure the sample temperature. These are located inside four sheaths penetrating and supported by the bottom ICF70 blank flange. The positions in the RC expressed as [radial position (mm), height (mm) from the bottom flange] are [10, 30], [0, 60], [10, 60] and [10, 90], respectively for RTD1, RTD2, RTD3 and RTD4.

The amount of H atom absorbed/adsorbed in the sample is deduced from decrease in the number of H_2 molecules calculated from pressure values at the storage tank (ST), P_s, and that at the RC, P_r, both measured with piezoelectric elements. Since one of the most important matters of concern is whether excess heat, if any, originates in nuclear effects or not, neutron and γ-ray counting rates are monitored steadily with a ^{3}He neutron dose rate meter and a NaI scintillation detector both located just outside the outer chamber.

All of the measured values mentioned above are processed with a "Measurement and Automation Explorer (MAX)" system, National Instruments. We are planning to make feedback control of the heater input power and the flow rate of the coolant to enable constant temperature operation in future.

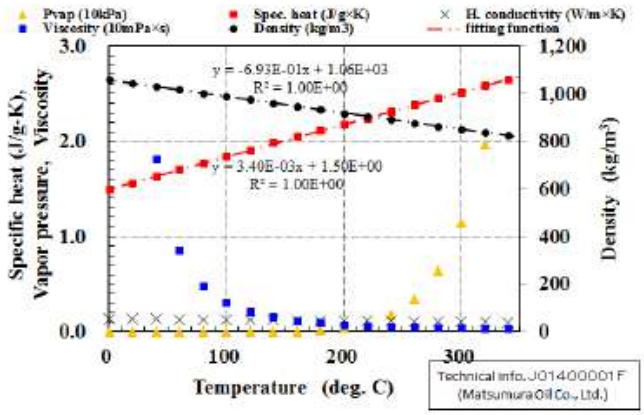

Figure 2. Physical properties of BarrelTherm-400.

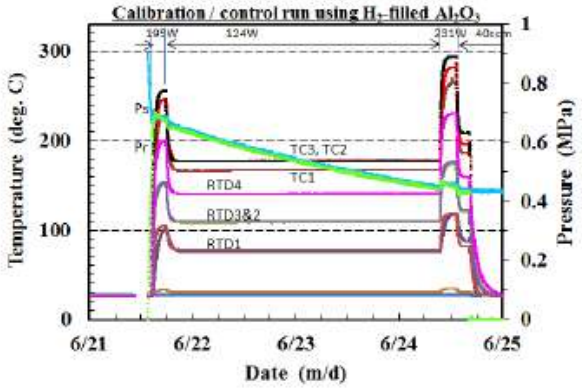

Figure 3. An example of functional fitting of the temperature change in the 195–124 W transition phase in the calibration run H–Al_2O_3.

The physical properties of the Barreltherm-400 are cited from Ref. [7], and shown in Fig. 2 as a function of temperature. It has rather strong temperature dependence of the viscosity. Although this might affect the flow rate of the coolant, the tubing pump is tough enough to send out the oil forcibly by the peristaltic rotors. The temperature dependence of the density and the specific heat are approximated by linear functions of temperature for the purpose of calculation of heat balance, etc.

3. Calibration

We have to know the heat conversion coefficient ($\mathrm{d}W/\mathrm{d}T$), the time constant (τ), and the heat recovery rate (R_h) beforehand using a dummy powder. We used a powder of alumina (Al_2O_3) with an average size of 60 μm for this purpose. Figure 3 shows temperature history during the calibration runs operated at heater input of 195, 124 and 231 W with a coolant flow rate of 20 and 40 cm^3/min.

After introduction of H_2 gas into the evacuated RC from the ST at [month/date hour:min] = [6/21 13:25], the pressures P_r and P_s begin to increase and decrease, respectively. The 195-W run was started at [6/21 14:22], when a discontinuous changes in pressure increase/decrease rate are observed as a result of temperature increase in the RC and resultant decrease in the pressure difference between the ST and the RC.

The heater power of 195 W was maintained for 3 h, during which the pressures and the temperatures reach almost saturated values. The power was changed to 124 W at [6/21 17:35], and a 231-W run followed at [6/24 9:16]. After about 4 h, the flow rate of the coolant was changed to 40 cm^3/min at [6/24 13:09]. This series of the calibration runs were finished by evacuating the RC at [6/24 16:05], followed by stopping the heater power supply at [6/24 16:20] and readjusting the flow rate to 20 cm^3/min at [6/24 16:26]. During the whole period of this calibration runs, the pressures P_s and P_r continue to decrease with almost constant rate. This should be due to some leak out of the ST–RC system. We have failed to fix it during the preliminary runs described in the following.

We see that the temperatures are very stable during the 2.5 days kept at 124 W; 178 $\pm$0.1°C at TC2 and 141 $\pm$0.07°C at RTD4. It is also important to note that the temperatures become almost saturated during each power phase with approximate time constant of 30 min. To calculate the heat conversion factor and the heat recovery rate, however, it is necessary to obtain the difference between each step as precise as possible. For this purpose, the temperature change is fitted to an exponential saturation function in each transition phase. An example of the fitting is shown in Fig. 4. Good fittings are obtained for both TC2 and RTD4.

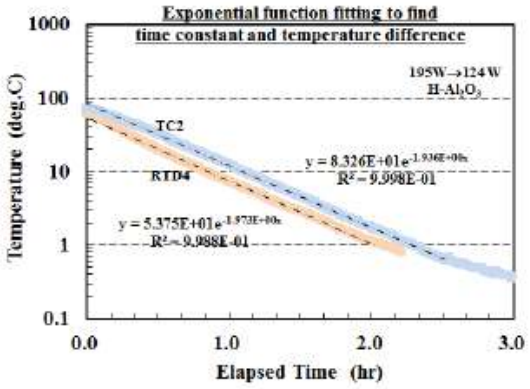

Figure 4. An example of functional fitting of the temperature change in the 195–124 W transition phase in the calibration run H–Al_2O_3.

The parameters thus deduced are summarized in Fig. 5 as a function of the input power. Although some dependence on the input power or the sample temperature could be deduced, we use in the following the average values; heat conversion coefficient dW/dT = (9.74 $\pm$0.76)$\times 10^{-1}$ W/°C, heat recovery rate R_h = (8.82 $\pm$0.26)$\times 10^{-1}$ with time constant τ = (2.98 $\pm$0.12)$\times 10^{1}$ min. Rather high value of the heat recovery rate is owing to high degree of thermal insulation for the RC.

4. Preliminary H-absorption run

A series of the trial runs have been conducted to find practical problems with use of a 50 g powder of silica-included Cu·Ni nano-composite, $Cu_{0.0071}Ni_{0.030}/SiO_2$ ("CNS", Admatechs Co. Ltd.), which contains 4.1 g of Ni (mostly as NiO) and 1.1 g of Cu with particle sizes of 5–50 nm in effective diameter. An EDS photograph shows that a part of the particles contains both Cu and Ni, implying that Cu and Ni atoms are merged into single particles to form some compounds.

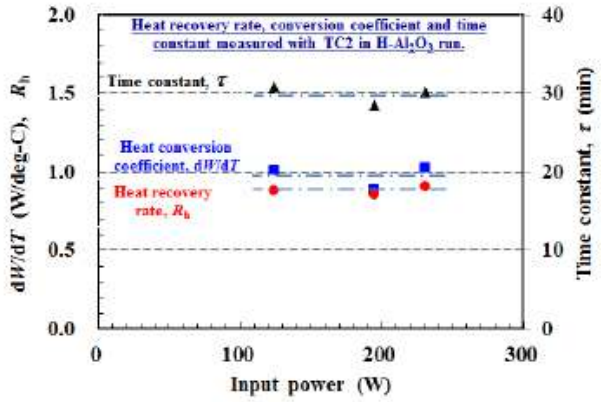

Figure 5. Heat conversion coefficient, recovery rate and time constant measured in the calibration run H–Al_2O_3.

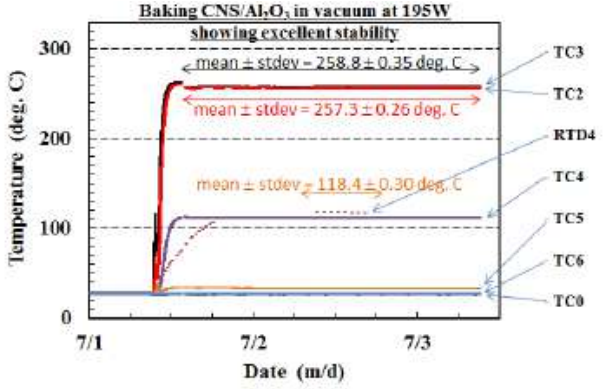

Figure 6. Baking process of the CNS/Al_2O_3 sample showing very stable temperatures everywhere in the system. The temperatures at RTD's were recorded manually in this period.

Since the 50 g sample of the CNS occupied only about 130 cm^3 in the RC volume, the RC was filled up with a mixture of the CNS and alumina that was used for the calibration/control run. The CNS/Al_2O_3 mixture was subjected first to vacuum baking at a heater input power of 196 W for about 2 days. The variation of the temperature during the baking process is shown in Fig. 6. Regrettably, due to a mis-setting of the RTD in the data acquisition system, we have the RTD data manually recorded for only several points.

The outer surface of the RC was kept at just below 260°C. In contrast, the sample temperature at RTD4 reached only 118°C even at the final stage of the baking process, when the pressure in the RC decreased down below 10^{-1} Pa. The reason for the relatively low temperatures at RTD's is relatively low heat conduction in the radial direction through the porous materials. In the case of the Al_2O_3 calibration run, H–Al_2O_3, we observed RTD4 showing 200°C, as has been described in the preceding section. This shows importance of the hydrogen gas at several atmospheres for heat conduction. Temperature, pressure and loading ratio in the run H–CNS/Al_2O_3.

Next we introduced hydrogen (protium) gas into the RC, and changed the heater input power from 195 W to 231

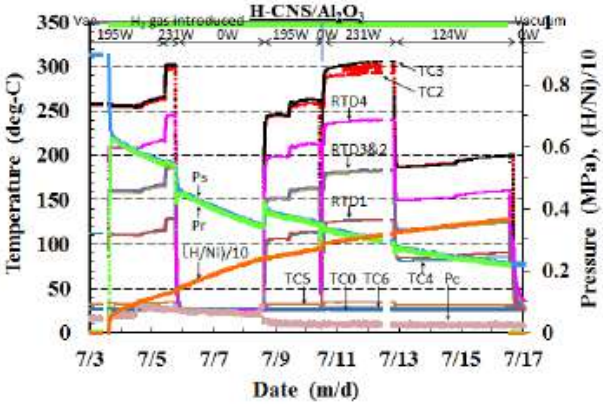

Figure 7. Temperature, pressure and loading ratio in the run H–CNS/Al_2O_3.

W, 0 W, 195 W and 231 W again, and finally to 124 W. The whole sequence of this run, H–CNS/Al_2O_3, is shown in Fig.7, where the traces of the temperatures, TC0–TC6 except TC1 and RTD1–RTD4, are shown together with the pressures, P_s, P_r, and P_c at the level monitor of BT400. Moreover, the amount of hydrogen atoms lost from the gas phase is shown as (H/Ni), the ratio of the number of the hydrogen atom absorbed/adsorbed to that of the host Ni atom, i.e., the so-called loading ratio. In the calculation of the number of hydrogen atoms in the gas phase from the measured pressures and temperatures together with the volumes of the ST and the RC, we assumed the representative temperature in the RC to be the mean temperature at RTD4 and TC3. Otherwise smooth variation of (H/Ni) was not reproduced.

The parameter (H/Ni) increases almost steadily throughout the whole run, which is thought to be caused by a leak out of the system as mentioned earlier. We also notice stepwise increases at the beginning when the gas is introduced into the RC, and just after the moment when the heater power is increased from 195 to 231 W. These should be due to real absorption/adsorption of hydrogen by the sample. Summing up the contributions, we obtain the loading ratio of 0.75 ± 0.05.

We notice that, in contrast to the control run H–Al_2O_3 shown in Fig. 3, the temperatures increase continuously under the constant input power of 195, 231 and 124 W. Moreover, almost stepwise increases are observed in the periods of 195 and 124 W. The increase was not observed in the control run H–Al_2O_3. As an example, the temperature evolutions in the 124 W phase of the H–CNS/Al_2O_3 run are compared with those of the H–Al_2O_3 run in Fig. 8. The comparison reveals temperature increase by 11–22°C at the TC2 and TC3, and by 9–20°C at the RTD4. If these increases can be attributed to the real increases in the power, they correspond to the "excess" powers of 11–22 W and 11–24 W, respectively. When evaluated in terms of the specific power, the "excess" amounts to about 5 W/g-Ni.

Similar values are deduced for the temperature increases in other periods of input power. Moreover, the assumed "excess" power is on the same order of magnitude as that claimed for the CNZ (Cu·Ni/Zi_2O_3) sample yielding an excess power of 2 W/g-Ni [6].

Before concluding there is excess power, we have to check for other possibilities. First, there might be a possibility that the temperature increase was due to a decrease in the flow rate of the coolant, which could be caused by a swelling of the coolant tube in the peristaltic pump tube section. Regarding this point, it should be noted that the Viton peristaltic pump tube was replaced by a Tygon one on July 8, after a leak in the Viton tube was found. We restarted the run with the new Tygon tube at a power of 195 W on the same day. It was not longer than one day before a similar temperature

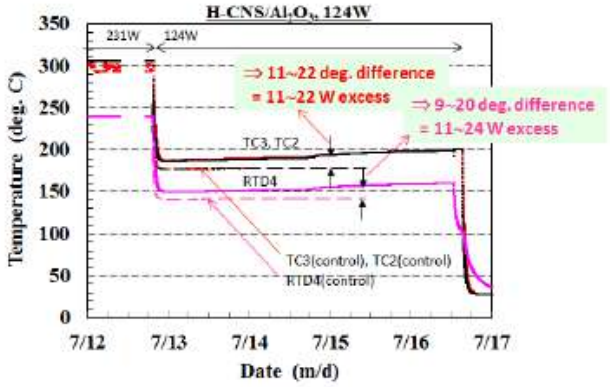

Figure 8. Comparison of the temperature change during the 124 W phase in the runs H–CNS/Al_2O_3 and H–Al_2O_3.

increase was observed. Therefore, it seems rather difficult to ascribe the temperature change to any deformation of the coolant tube.

Another possibility could be a transformation of the sample itself due to repeated cycle of heating. Agglomeration of the Cu·Ni particles or interwinding of the two kinds of the powders might occur. Both of these changes could increase the thermal conductivity of the sample to make the thermal flow from the heater to the sample bulk higher and raise the sample temperature. However, it appears to be difficult to explain by this mechanism the temperature increases at TC2 through TC4 by almost the same values as those at RTD1 through RTD4.

The system has a gas leak which could affect the calorimetry, since the heat transfer due to thermal conduction and/or convection, or heat loss via the top and bottom flanges, becomes less active as the pressure decreases. This effect is negligible in the present configuration, since the effect would cause a temperature decrease (not an increase) at the RTD's with decreasing pressure, since the RTD's are located near the heat sink. Moreover, we are comparing the temperature evolutions in the foreground (CNS) runs with those in the background (Al_2O_3) runs which also have the gas leak out of the system with a rate of the same order of magnitude as shown in Fig. 3.

Finally, we have to mention that no noticeable change was observed in either the γ-ray or the neutron counting rates, as is shown in Fig. 9. The heater power calculated from the measured voltage across the heater and the resistance at room temperature is also plotted in the figure. It is also clear that the fluctuation of the input power is not the origin of the temperature increases.

In short, it is reasonably plausible to ascribe the observed temperature increase to excess power from the sample. It is, however, also true that the increased amount is too small to rule out all other factors which could affect the temperature. We have designed the calorimeter system to hold an increased amount of the sample material, of the order of several hundred grams. Unfortunately, only 50 g of the CNS sample containing only 4.1 g of the active element Ni is available at the moment. We are planning to test the CNZ sample with an amount on the order of 100 g.

5. Conclusion

As for the calibration of the oil-mass-flow calorimetry using a dummy Al_2O_3 powder, we summarize the results as follows:

(A1) The coolant oil reached almost 300°C at the input heater power of 231W.

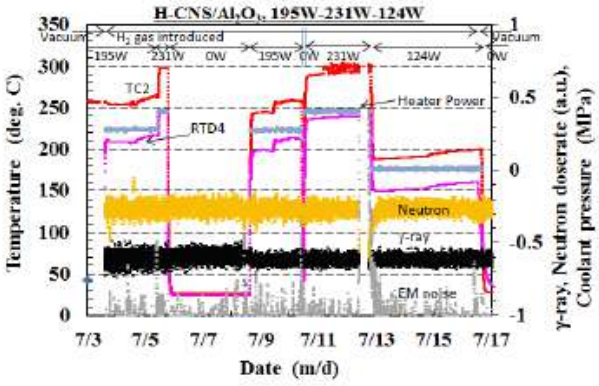

Figure 9. Neutron and γ-ray signals as well as heater power in the H–CNS/Al_2O_3 run, showing no relation between these and the temperature change.

(A2) Long-term stability, or fluctuation in terms of standard deviation, is better than 0.5°C.
(A3) Conversion coefficient, dW/dT = (0.97 ±0.08) W/deg with an oil-flow rate of 20 cm^3/min.
(A4) Heat recovery efficiency is (0.88 ±0.03) with heat removal time constant of (30 ±1.2) min.

The first trial runs with a 50 g of the CNS sample (silica-included Cu·Ni nano-compound containing 4.1 g of Ni) mixed with 200 g of Al_2O_3 are summarized with the following remarks:

(B1) Both TC2 at the oil outlet and RTD's inside the reaction chamber show higher temperatures than those for the blank sample, which could imply a long-lasting excess power of 20 W (i.e., 5 W/g-Ni).
(B2) The assumed excess heat appears to be on the same order as that of the CNZ (Cu·Ni/Zi2O3) sample yielding an excess power of 2 W/g-Ni.
(B3) Further measurements with increased amount of the sample and more precise comparison are necessary to confirm the excess power.

Acknowledgement

The authors thank Admatechs Co. Ltd. for providing the CNS sample and its TEM, EDS, ICP and XRD analyses.

References

[1] Akira Kitamura, Yu Sasaki, Yuki Miyoshi, Akira Taniike, Akito Takahashi, Reiko Seto and Yushi Fujita, *J. Condensed Matter Nucl. Sci.* **4** (2011) 56–68.
[2] Y. Miyoshi, H. Sakoh, A. Taniike, A. Kitamura, A. Takahashi, R. Seto and Y. Fujita, *J. Condensed Matter Nucl. Sci.* **10** (2013) 46–62.
[3] Y. Miyoshi, H. Sakoh, A. Taniike, A. Kitamura, A. Takahashi, R. Seto and Y. Fujita, *Proc. JCF12* (2012) 1–9.
[4] H. Sakoh, Y. Miyoshi, A. Taniike, Y. Furuyama, A. Kitamura, A. Takahashi, R. Seto, Y. Fujita, T. Murota, T. Tahara, to be published.
[5] H. Sakoh, Y. Miyoshi, A. Taniike, Y. Furuyama, A. Kitamura, A. Takahashi, R. Seto, Y. Fujita, T. Murota, T. Tahara, *Proc. JCF13*.
[6] A. Takahashi, A. Kitamura, R. Seto, Y. Fujita, H. Sakoh, Y. Miyoshi, A. Taniike, Y. Furuyama, T. Murota and T. Tahara, to be published.
[7] Technical info. J01400001F (Matsumura Oil Co. Ltd.).